First gas-phase generation of a *cis* chloroiminoarsane $\mathrm{ClAs{=}NSiMe_3}$ and a *cis* chloroiminophosphane $\mathrm{ClP{=}NSiMe_2{}^tBu}$. Characterization by photoelectron spectroscopy[†]

Karinne Miqueu, Jean-Marc Sotiropoulos, Genevieve Pfister-Guillouzo* and Vadim D. Romanenko

Laboratoire de Physico-Chimie Moléculaire (CNRS UMR 5624), Université de Pau et des Pays de l'Adour, Avenue de l'Université, F-64000 Pau, France. E-mail: genevieve.pfister@univ-pau.fr; Fax: +33 (0) 5 59 50 83 44

Received (in Montpellier, France) 27th February 2001, Accepted 4th May 2001
First published as an Advance Article on the web 19th June 2001

Photoelectron spectroscopy-flash vacuum thermolysis in the gas phase allowed us to synthesize, for the first time, the *cis* forms of two weakly hindered, low-coordinate arsenic and phosphorus compounds ($\mathrm{ClPn{=}NSiR_3}$; Pn = P, As), as well as to characterize them by their ionization energies. In order to assign the different bands in the PE spectra and to estimate the effect of the substituents $\mathrm{SiMe_3}$ and Cl on the electronic and structural properties of these compounds, we performed calculations using density functional theory (hybrid functional B3LYP) with the basis set 6-311G(d,p). The thermodynamic stabilization of these halogenated systems appears in the important antiperiplanar interactions between the nitrogen lone pair n_N and the σ^*_{AsCl} (or σ^*_{PCl}) orbital. For these two compounds, in spite of a poor $2p\pi(N)$–$3p\pi(P)/4p\pi(As)$ overlap, it was observed that the substitution of a chlorine atom on the pnictogen (As, P) and a silyl group on nitrogen (negative hyperconjugation) leads to a relatively high ionization energy for the $\pi_{Pn{=}N}$ orbital [$\mathrm{IE}(\pi_{Pn{=}N}) \approx 10$ eV].

Première synthèse en phase gazeuse d'une *cis* chloro-arsa-imine $\mathrm{ClAs{=}NSiMe_3}$ et d'une *cis* chloro-phospha-imine $\mathrm{ClP{=}NSiMe_2{}^tBu}$. Caractérisation par spectroscopie photoélectronique. Une étude expérimentale en phase gazeuse (spectroscopie photoélectronique-couplage thermolyse éclair) nous a permis de synthétiser, pour la première fois, deux composés monomériques à basse coordinence de l'arsenic et du phosphore peu encombrés ($\mathrm{ClPn{=}NSiR_3}$; Pn = P, As) sous leur forme *cis* ainsi que de les caractériser par leurs potentiels d'ionisation. Pour attribuer les differentes ionisations sur les spectres photoélectroniques et estimer l'effet des substituants Cl et $\mathrm{SiMe_3}$ sur les propriétés électroniques et structurales de ces composés, nous avons réalisé une étude théorique en utilisant la théorie de la fonctionnelle de la densité (fonctionnelle hybride B3LYP) et la base 6-311G(d,p). La stabilisation thermodynamique de ces dérivés halogénés est essentiellement due à la présence d'interactions entre la paire libre de l'azote n_N et l'orbitale vacante σ^*_{AsCl}. Pour ces deux composés, malgré un mauvais recouvrement $2p\pi(N)$–$3p\pi(P)/4p\pi(As)$, la substitution par un atome de chlore sur l'atome de pnictogene (As, P) ainsi que la présence d'un groupement silyl sur l'azote (hyperconjugaison négative) entrainent une stabilisation de l'ionisation associée à l'orbitale $\pi_{Pn{=}N}$ [$\mathrm{EI}(\pi_{Pn{=}N}) \approx 10$ eV].

The low-coordination number chemistry of the group 15 elements (N, P, As) has been extensively developed in the past few years thanks to the use of bulky groups.[2] It has been possible to characterize these reactive species due to their kinetic and thermodynamic stabilization by appropriate substitution. Another approach to the study of such molecules involves the use of well-established techniques: gas-phase generation by flash vacuum thermolysis (FVT) or vacuum gas–solid reactions (VGSR) coupled with mass spectrometry or UV photoelectron spectroscopy (UV-PES). For example, many iminophosphanes, mainly substituted with bulky and/or amino groups, have been described in the literature[2a,b,3] whereas few experimental results have been reported on the corresponding arsenic derivatives.[4] At present, only *trans* iminoarsanes with bulky substituents have been isolated[4] and the main information available concerns their synthesis and X-ray structure. Recently, we synthesized by FVT less hindered *trans* aminoiminoarsanes and iminophosphanes and characterized them by UV-PES.[5] This was the first report on the electronic properties of such compounds.

Most of these compounds are known in their *trans* form, however, only very few *cis* hindered iminophosphanes have yet been synthesized. The main examples concern the halogenated iminophosphanes $\mathrm{XP{=}NMes^*}$ (X = I, Br, Cl).[6] For such chlorinated systems, the preference for the *cis* form is in agreement with quantum chemical calculations.[7] Indeed, it has been shown that the σ electron push–pull substitution [phosphorus atom substituted with a withdrawing group (Cl, F), nitrogen atom with a σ electron-releasing substituent ($\mathrm{SiH_3}$)] leads to the lowest energy *cis* form.

The aim of this work was to generate by FVT the highly reactive *cis* chloroiminoarsane $\mathrm{ClAs{=}NSiR_3}$ and chloroiminophosphane $\mathrm{ClP{=}NSiR_3}$, as well as to characterize these short-lived species by UV-PES. The thermolysis of $\mathrm{Cl_2PnN(SiR_3)_2}$ (Pn = As, P) was envisaged in order to generate the expected $\mathrm{ClPn{=}NSiR_3}$ by loss of chlorosilane. The latter is a good leaving group in thermal decomposition reactions and such a method is often used to synthesize low-coordinate compounds.

[†] Application of photoelectron spectroscopy to molecular properties. Part 61. For part 60, see: ref. 1.

Experimental results

Precursors

We chose as one SiR_3 substituent $SiMe_3$ because it is the least bulky silylated group usually used in synthesis. We also used $SiMe_2{}^tBu$ in order to stabilize the precursors. $Cl_2PN(SiMe_3)_2$ (**1a**) is only stable in solution and so its characterization by UV-PES was impossible. In contrast, the arsenic analog $Cl_2AsN(SiMe_3)_2$ (**1b**) can be prepared and studied in the gas phase. We have also synthesized two other precursors, $Cl_2PN(SiMe_2{}^tBu)_2$ (**2a**) and $Cl_2AsN(SiMe_2{}^tBu)_2$ (**2b**), which are more stable than **1a** and **1b**. For **2a** and **2b**, two competitive reactions can occur (Scheme 1) during the thermolysis: $Me_2{}^tBuSiCl$ elimination (path 1) and/or thermic fragmentation of the *tert*-butyl group along with loss of isobutene and HCl (path 2). We only present here the photoelectronic spectra recorded below 773 K which corresponds to the first elimination. Indeed, above 773 K the spectra are too complex since there is a competition between the two fragmentation pathways (observation of the loss of isobutene, HCl, $Me_2{}^tBuSiCl$).

UV Photoelectron spectra

There is a notable similarity between the UV-PES spectra of **1b** and **2b** (Fig. 1). The first two bands are respectively observed at 9 (**1b**) and 8.6 (**2b**), and at 9.5 (**1b**) and 9.4 eV (**2b**). The subsequent, more intense bands, appear between 11 and 13 eV.

The energetically preferred structure, calculated for the less bulky compound $Cl_2AsN(SiH_3)_2$ at the B3LYP/6-311G(d,p) level presents an orthogonal orientation of the nitrogen and arsenic lone pairs [N sp^2, As sp^3 ($\Sigma\hat{A}s = 298°$)].

The first ionic state, calculated to lie at 9.84 eV, is associated with the ionization of the amino nitrogen lone pair (first band) and the second, calculated to be at 10.18 eV, with the ionization of the arsenic lone pair (second band). For **2b**, this more intense, second band, also overlaps the ionizations of the σ_{SiC} orbital electrons. The positions of the experimental bands are in good agreement with the calculated energies (taking into account the effect of substituents).

The spectrum of $Cl_2PN(SiMe_2{}^tBu)_2$ [Fig. 2(a)] shows three first ionizations at 9, 9.7 and 10.6 eV, followed by two broad and intense bands centered on 11.4 and 12.9 eV. In order to assign these ionizations, we performed a calculation on $Cl_2PN(SiH_3)_2$. As for $Cl_2AsN(SiH_3)_2$, the lowest energy structure corresponds to the form with the phosphorus (P sp^3) and the nitrogen (N sp^2) lone pairs orthogonal, but in this case, the s character of the phosphorus lone pair is less important ($\Sigma\hat{P} = 303°$). The first ionic state, computed to be at 9.76 eV, corresponds to the ejection of an electron from the phosphorus lone pair. It is 0.42 eV below that of the arsenic lone pair (10.18 eV), which is in agreement with the previous observation concerning the s character. Thus, taking into account the destabilizing effect of the methyl and the *tert*-butyl groups, as well as the proximity of the two Kohn–Sham orbitals for $Cl_2PN(SiH_3)_2$, the first band at 9 eV overlaps the ionizations of the nitrogen and phosphorus lone pair electrons and the band at 9.7 eV corresponds to the ionization of the σ_{SiC} orbital electrons.

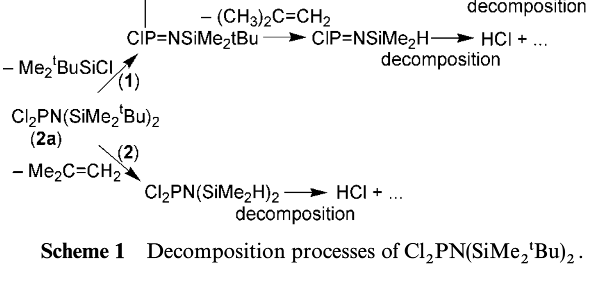

Scheme 1 Decomposition processes of $Cl_2PN(SiMe_2{}^tBu)_2$.

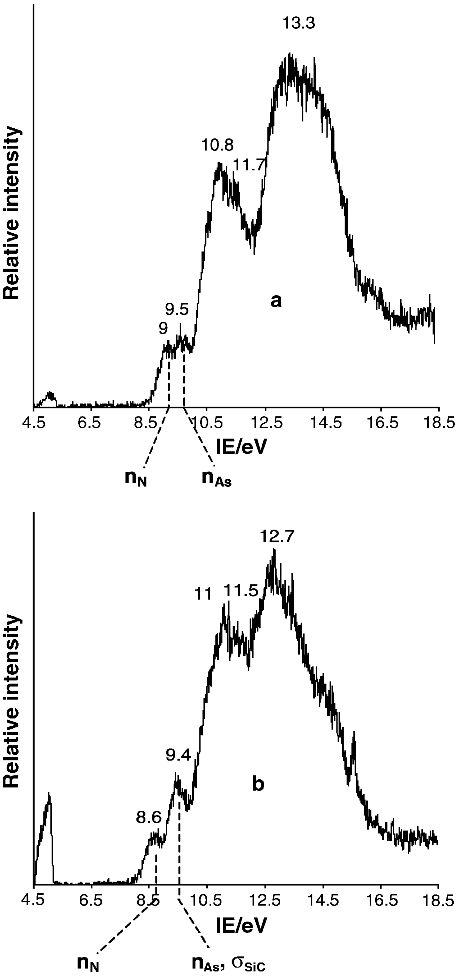

Fig. 1 UV-PES spectra of the precursors (a) $Cl_2AsN(SiMe_3)_2$ (**1b**) at 320 K and (b) $Cl_2AsN(SiMe_2{}^tBu)_2$ (**2b**) at 340 K.

Thermolysis photoelectron spectra

The spectrum of $Cl_2AsN(SiMe_2{}^tBu)_2$ (**2b**) appears to be slightly modified from 693 K onwards. The flash vacuum thermolysis was incomplete and it was impossible to correctly assign the ionizations. On the contrary, for $Cl_2PN(SiMe_2{}^tBu)_2$ (**2a**), the first characteristic band of the precursor (9.0 eV) disappears at 593 K, showing complete cleavage of **2a**. During the thermolysis, when the oven is inside the spectrometer, the first new band appears at 9.6 eV and is broad, then a shoulder at 10.6 eV is followed by two broad bands at 11.7 and 13.1 eV [Fig. 2(b)]. Moreover, $(CH_3)_2{}^tBuSiCl$ (Scheme 1) was the only volatile and stable compound generated during a separate study of the pyrolysis products (in this case the oven is outside the spectrometer and only long-lived molecules are detected; see Experimental for a detailed description of the thermolysis experiments). Thus, these ionizations can be assigned to a new species, $(CH_3)_2{}^tBuSiCl$, whose characteristic ionizations are 9.6 and 10.6 eV. The PE spectrum at 593 K [Fig. 2(d)] obtained after subtraction of the PE spectrum of $(CH_3)_2{}^tBuSiCl$ displays a first broad band centered at 9.3 eV and two others centered on 10.5 (with a shoulder at 10.2 eV) and 11.1 eV.

The spectrum of $Cl_2AsN(SiMe_3)_2$ (**1b**) changes up to 773 K [Fig. 3(a), Scheme 2]. At this temperature, the disappearance of the bands between 11 and 11.7 eV (chlorine lone pairs) is observed, indicating complete thermolysis of the precursor. The new spectrum shows the characteristic ionizations of

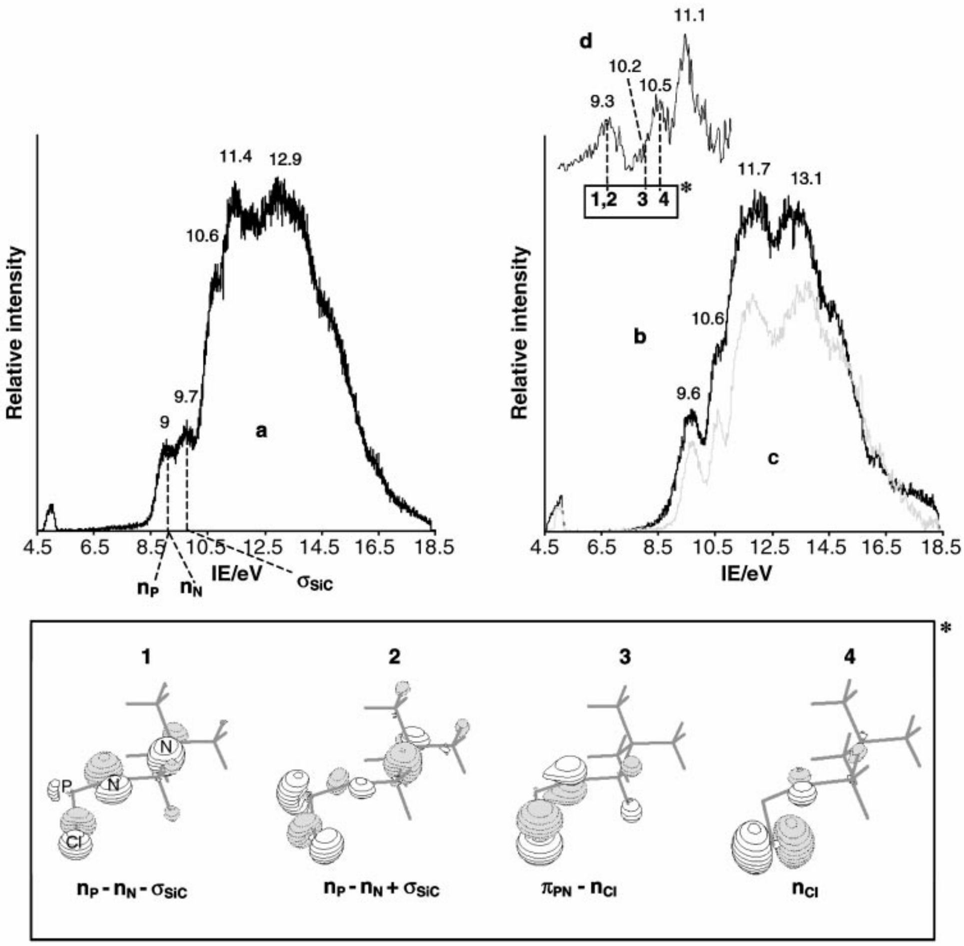

Fig. 2 (a) UV-PES spectrum of the precursor $Cl_2PN(SiMe_2{}^tBu)_2$ (**2a**) at 340 K. (b) Thermolysis spectrum of **2a** at 593 K. (c) Spectrum of $Me_2{}^tBuSiCl$ at 300 K. (d) Difference between spectra b and c.

Me_3SiCl at 10.6 and 11.9 eV (loss confirmed by trapping) and three lower energy bands at 9.2, 9.8 and 10.6 eV.

At higher temperatures (1223 K) we observe another spectrum [Fig. 3(b)] with a broad band at 8.9 eV and a second at 10.6 eV with a shoulder at 9.8 eV. This spectrum is identical to that recorded from the thermolysis of $ClAs[N(SiMe_3)_2]_2$ at 773 K. In this latter case, we principally observed, by external thermolysis, the elimination of $N(SiMe_3)_3$ (Scheme 2). The loss of amine is in agreement with the previous work of Niecke and Bitter.[8] They studied, in solution, the thermolysis reaction of $ClAs[N(SiMe_3)_2]_2$ and observed the formation of $N(SiMe_3)_3$ as well as a polymeric species, $(ClAsNSiMe_3)_n$.

For the two thermolysis reactions of **2a** and **2b**, the loss of Me_3SiCl or $Me_2{}^tBuSiCl$ allows us to conclude that monomeric $ClPn{=}NSiR_3$ or dimeric $(ClPNSiR_3)_2$ species are formed. Elbel has shown previously that the thermolysis of the [2 + 1] dimer of $^tBuP{=}N^tBu$ gives the monomer[9a] but, in contrast, Walther[9b] has shown that the [2 + 2] $(ClPN^tBu)_2$ dimer is thermically stable and no monomer was observed during the thermolysis. By taking into account this observation we conclude that, if a dimeric species is generated it will be the [2 + 2] dimer and not the [2 + 1]. Thus, in order to interpret the different experimental results and to assign the new spectra, we performed calculations on $ClAs{=}NSiMe_3$, $ClP{=}NSiH_2{}^tBu$, $ClP{=}NSiMe_2H$ and on dimeric species with less bulky substituents, $(ClPnNSiH_3)_2$ [Pn = As, P].

Theoretical results

We carried out calculations on different iminoarsanes in order to determine the preferred structures. As for the iminophosphanes, we checked that the substitution on arsenic of a chlorine atom and/or on nitrogen of a silyl group led to the *cis* form as the lowest energy structure. The three less substituted compounds $R_1As{=}NR_2$ [$R_1 = R_2 = H$; $R_1 = Cl$, $R_2 = H$; $R_1 = H$, $R_2 = SiH_3$] present two minima (*cis* and *trans* forms) on the potential energy surface. For $ClAs{=}NSiH_3$ [$R_1 = Cl$, $R_2 = SiH_3$], the only minimum found was the *cis* form. The *trans* form of the parent compound HAs=NH is calculated to be only slightly more stable than the *cis* form. The difference in energy of 0.4 kcal mol^{-1} is negligable, indicating no preference for the *cis* or *trans* isomers. On the contrary, for all the other compounds [$R_1 = H$, Cl; $R_2 = H$, SiH_3] the *cis* form is the more energetically stable, in spite of the lesser importance of the electronic energy in this form than in the *trans* isomer. Consequently, the nuclear energy seems to play a dominant role. This observation is interesting since, until now, only antiperiplanar stabilizing interactions were suggested to explain the *cis* form as the lowest energy structure.[2a] From Table 1 (E_{elec}, E_{rep}) and the information obtained from NBO[10] calculations, we can explain this result. Indeed, for the *cis* form of the iminoarsanes, the NBO population analysis shows the presence of antiperiplanar stabilizing interactions between the arsenic lone pair and the σ^*_{NR2} orbital and between the nitrogen lone pair and the empty σ^*_{AsR1} orbital. These interactions are very strong for the halogenated derivatives, especially the $n_N \rightarrow \sigma^*_{AsR1}$, and are more important in the *cis* form. Thus, highly destabilizing interactions involving four electrons probably counterbalance these stabilizing interactions since the electronic energy is always less important for the *cis* isomer than for the *trans* form. Consequently, the stability of the preferred structure can be explained not

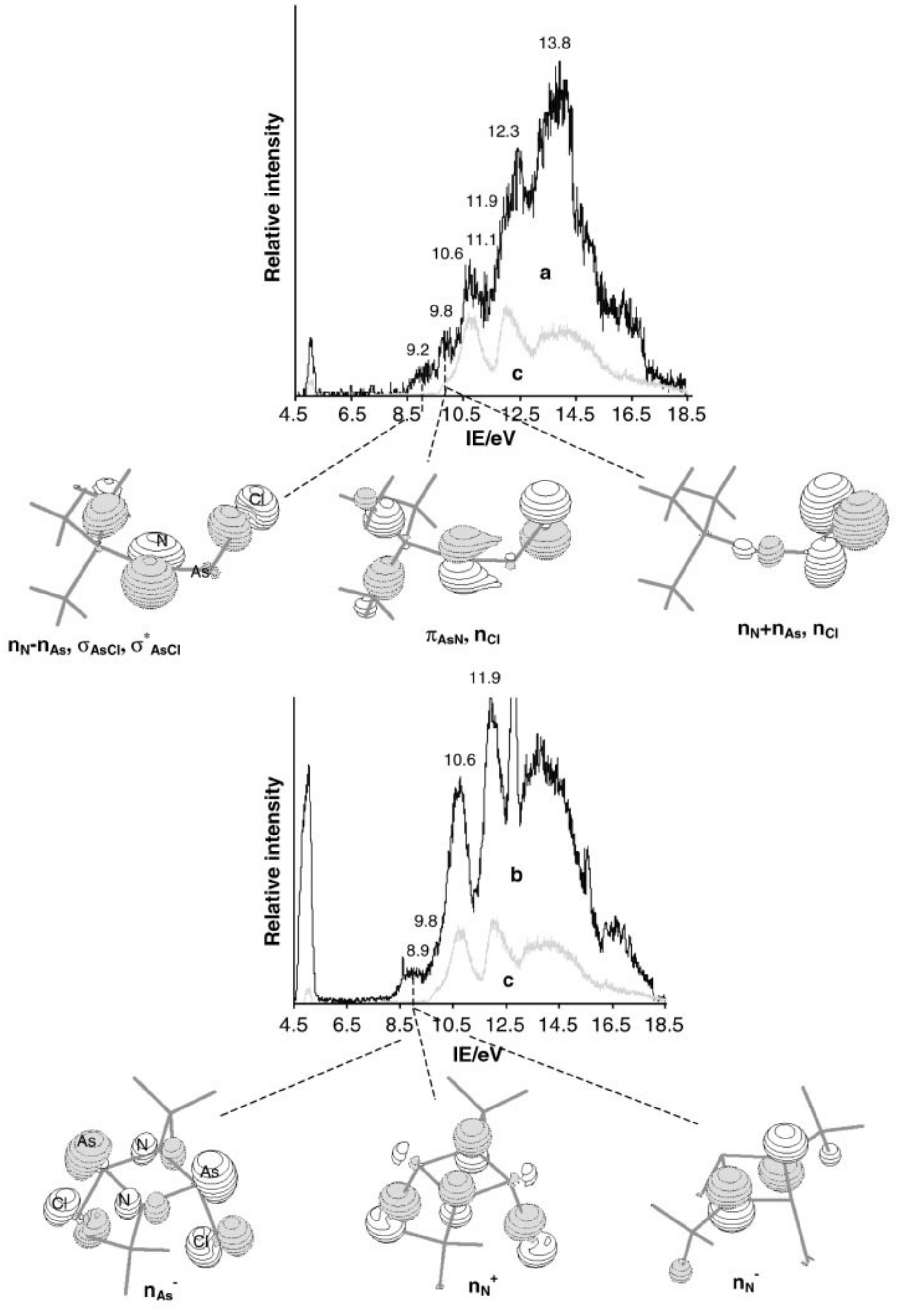

Fig. 3 Thermolysis spectra of **1b** at (a) 773 and (b) 1223 K. (c) Spectrum of Me_3SiCl at 300 K.

only by interactions between an occupied and a virtual orbital but also by a weak nuclear repulsion. This conclusion is in agreement with the observed geometrical modifications. Indeed, whatever the substitution on arsenic and nitrogen, an opening of the bond angles (Table 2) can be seen for the *cis* isomer, bringing about a minimization of the nuclear repulsion energy.

The geometrical parameters are influenced by the conformation of the compound and especially by the substituents linked to As and N (Table 2). For the parent compound HAs=NH, the two bond angles HAsN and AsNH are larger in the *cis* conformation than in the *trans* form. The As=N bond length is about 1.7 Å for both structures but slightly shorter in the *cis* isomer, which is in agreement with the opening of the bond angles. Obviously, when nitrogen is substituted with an electropositive group (SiH_3), the s character on the nitrogen lone pair decreases and thus the As=N bond is shortened and the AsNSi bond angle is opened. It is well known that the p character of the nitrogen lone pair increases when N-silylation occurs. But, in the same way, the electronegativity[11] (Allred–Rochow electronegativity) of the heteroatom in the α position to nitrogen induces a change in the hybridization. Actually, X-ray experiments show angles of 177.8 and 136.0°, respectively, for *N*-silyl silanimine[12] (χ_{Si} 1.74) and germanimine[13] (χ_{Ge} 2.02) moieties. Calculations give the same conclusions [in $(CH_3)_2X{=}NSiH_3$ the XNSi angle is 166.5 and 133.4° for $X = Si$ and Ge, respectively].[14] For the arsaimine $HAs{=}NSiH_3$ (χ_{As} 2.20) the computed angle is 132.51° for the *cis* isomer and 128.19° for the *trans* conformation.

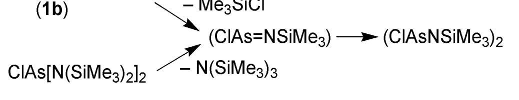

Scheme 2 Decomposition processes of $Cl_2AsN(SiMe_3)_2$ and $ClAs[N(SiMe_3)_2]_2$.

Table 1 Calculated energies for the *cis* and *trans* forms of $R_1As{=}NR_2$, including the nuclear repulsion (E_{rep}) and electronic (E_{elec}) energies, the energy difference between the two isomers (E_{c-t}) and the principal stabilization energies ($n \rightarrow \sigma^*$)

R_1		H	H	Cl	Cl[a]	Cl[a]
R_2		H	SiH_3	H	SiH_3	$SiMe_3$
E_{elec}/a.u.	*cis*	−2387.205 614	−2810.573 940	−2988.724 424	−3439.607 820	−2450.527 916
	trans	−2387.165 663	−2811.061 300	−2991.209 865	—	—
$n_N \rightarrow \sigma^*_{AsR1}$/kcal mol^{-1}	*cis*	5.11	7.93	15.25	22.85	26.32
	trans	3.50	5.34	5.98	—	—
$n_{As} \rightarrow \sigma^*_{NR2}$/kcal mol^{-1}	*cis*	2.04	6.55	3.56	9.05	8.42
	trans	—	3.75	—	—	—
E_{rep}/a.u.	*cis*	95.407 460	228.033 058	237.246 809	397.383 942	709.720 962
	trans	95.366 866	228.522 109	239.739 863	—	—
E_{c-t}/kcal mol^{-1}		0.40	−1.06	−4.78	—	—

[a] For these compounds, only the *cis* form is a minimum on the potential energy surface.

The chlorine atom on As also leads to a shortening of the As=N double bond and to opening of the nitrogen angle. In fact, the shortest AsN double bond length is obtained for $ClAs{=}SiMe_3$. For this compound, the *cis* form presents an AsN bond length about 1.651 Å and bond angles at As and N of 110 and 152°, respectively.

In order to compare iminoarsanes and iminophosphanes, we extended our calculations to several $R_1P{=}NR_2$ species [$R_1 = H$, $R_2 = SiH_3$; $R_1 = Cl$, $R_2 = H$, SiH_3, $SiMe_3$, $SiHMe_2$, $SiH_2{}^tBu$]. Niecke *et al.*[7] also studied some of these [$R_1 = H$, $R_2 = SiH_3$; $R_1 = Cl$, $R_2 = H$, SiH_3] but did not use the DFT method (calculations were carried out at the SCF level using a double-ξ quality basis set). For HP=NH, the *trans* isomer is more stable than the *cis* form by about 0.4 kcal mol^{-1} while for all the other studied iminophosphanes the *cis* form is the preferred structure (Table 3). The compounds with a Cl atom on phosphorus and an SiR_3 group on nitrogen present only one minimum: the *cis* isomer. For ClP=NH, the most stable form corresponds to that with the weakest nuclear repulsion energy, whereas for $HP{=}NSiH_3$, it is that with the greatest electronic energy (Table 3). The comparison between iminoarsanes (Table 1) and iminophosphanes (Table 3) shows that the stabilizing interactions are more important for the phosphorus compounds than for the arsenic ones. This observation can be explained by the fact that the 2pπ(N)–3pπ(P) overlap is better than that of 2pπ(N)–4pπ(As).

As for the iminoarsanes, the variation in substituents R_1 and R_2 on $R_1P{=}NR_2$ causes considerable changes in geometry (Table 4). For instance, calculations carried out with the $SiH_2{}^tBu$ group show that the P=N (1.517 Å) bond length is very short and the nitrogen bond angle rather open (159°).

In order to estimate the expected ionization energies for $ClAs{=}NSiMe_3$ and $ClP{=}NSiMe_2{}^tBu$ we performed a direct calculation of the first two ionic states (ΔSCF calculations). To model $ClP{=}NSiMe_2{}^tBu$, the calculations were carried out on two systems with less bulky substituents [$ClP{=}NSiH_2{}^tBu$, $ClP{=}NSiMe_2H$]. We present in Table 5 the calculated ionization energies and also the Kohn–Sham energies for $ClP{=}NR_2$ ($R_2 = SiMe_3$, $SiHMe_2$, $SiH_2{}^tBu$) and for $ClAs{=}NR_2$ ($R_2 = SiMe_3$).

For all these systems, the first ionic state (A′) is associated with the removal of an electron from the pnictogen and nitrogen antibonding combination of lone pairs mixed with the σ_{PnCl} and σ^*_{PnCl} orbitals. For this molecular orbital, an important localization on the nitrogen and chlorine atoms is noted. The second ionic state (A″) corresponds to the ionization of a π electron. The main difference between the arsenic and phosphorus systems is the ionization energy of this A″ ionic state.

Table 2 Calculated geometrical parameters for the *cis* and *trans* forms of $R_1As{=}NR_2$

R_1		H	H	Cl	Cl	Cl
R_2		H	SiH_3	H	SiH_3	$SiMe_3$
As=N/Å	*cis*	1.712	1.698	1.672	1.656	1.651
	trans	1.722	1.706	1.692	—	—
R_1AsN/°	*cis*	103.37	102.92	109.22	109.59	110.281
	trans	95.84	97.92	100.87	—	—
$AsNR_2$/°	*cis*	113.41	132.51	121.54	146.85	151.785
	trans	107.47	128.19	110.23	—	—

Table 3 Calculated energies for the *cis* and *trans* forms of $R_1P{=}NR_2$, including the nuclear repulsion (E_{rep}) and electronic (E_{elec}) energies, the energy difference between the two isomers (E_{c-t}) and the principal stabilization energies ($n \rightarrow \sigma^*$)

R_1		H	H	Cl	Cl[a]	Cl[a]	Cl[a]	Cl[a]
R_2		H	SiH_3	H	SiH_3	$SiMe_2H$	$SiMe_3$	$SiH_2{}^tBu$
E_{elec}/a.u.	*cis*	−446.929 394	−825.003 606	−986.038 421	−1392.968 778	−818.768 201	−757.258 453	−711.609 368
	trans	−446.859 272	−824.984 842	−987.983 003	—	—	—	
$n_N \rightarrow \sigma^*_{PR1}$/kcal mol^{-1}	*cis*	7.62	11.68	22.50	34.93	36.35	37.73	36.03
	trans	4.87	8.09	8.51	—	—	—	—
$n_P \rightarrow \sigma^*_{NR2}$/kcal mol^{-1}	*cis*	3.51	7.54	5.79	9.19	8.27	8.27	9.55
	trans	—	3.44	—	—	—	—	—
E_{rep}/a.u.	*cis*	49.626 277	136.956 370	129.060 143	245.241 999	407.642 970	508.494 172	593.425 164
	trans	49.555 520	136.939 614	131.013 670	—	—	—	—
E_{c-t}/kcal mol^{-1}		0.40	−1.93	−5.61	—			

[a] For these compounds, only the *cis* form is a minimum on the potential energy surface.

Table 4 Calculated geometrical parameters for the *cis* and *trans* forms of $R_1P{=}NR_2$

R_1 R_2		H H	H SiH_3	Cl H	Cl SiH_3	Cl $SiMe_2H$	Cl $SiMe_3$	Cl $SiH_2{}^tBu$
P=N/Å	*cis*	1.574	1.559	1.530	1.518	1.518	1.516	1.517
	trans	1.588	1.566	1.553	—	—	—	—
R_1PN/°	*cis*	105.95	105.38	111.55	111.25	111.58	111.68	111.31
	trans	98.77	101.47	104.04	—	—	—	—
PNR_2/°	*cis*	118.52	139.95	131.00	158.25	157.46	159.04	159.15
	trans	109.79	135.53	115.11	—	—	—	—

It is lower for the iminoarsanes compared to the iminophosphanes because of the more diffuse character of the $\pi_{As=N}$ double bond.

For all these compounds, in spite of the poor 2pπ(N)–3pπ(P)/4pπ(As) overlap, the substitution of a chlorine atom on the pnictogen (As, P) involves a relatively high $\pi_{Pn=N}$ orbital ionization energy compared to iminophosphanes and/or arsanes,[2b,3,5] since calculated values are about 10 eV. By taking into account the Kohn–Sham orbitals, we can estimate the order of the subsequent ionizations. The third Kohn–Sham orbital, which is the bonding combination of the lone pairs mixed with the *peri*-chlorine lone pair (high weight on arsenic and chlorine atoms), lies very close to the second. Indeed, the difference between the Kohn–Sham energy of the *peri*-chlorine lone pair and this $\pi_{Pn=N}$ orbital is less than 0.2 eV, while the gap between these orbitals and the following

Table 5 Calculated Kohn–Sham energies, ionic state energies and assignment of the molecular orbitals for the $ClPn{=}NSiR_3$ (Pn = As, P) *cis* isomers

$ClAs{=}NSiMe_3$	$ClP{=}NSiMe_3$	$ClP{=}NSiHMe_2$	$ClP{=}NSiH_2{}^tBu$
Kohn–Sham energies (in eV) and assignment of molecular orbitals			
−7.47 $n_N - n^{\sigma}_{Cl}$	−7.49 $n_N - n_P - n^{\sigma}_{Cl}$	−7.62 $n_N - n_P - n^{\sigma}_{Cl}$	−7.54 $(n_N - n_P) - n_{Cl} - \sigma_{SiC}$
−7.92 $\pi_{As=N} - n^{\pi}_{Cl}$	−8.17 $\pi_{P=N} - n^{\pi}_{Cl}$	−8.29 $\pi_{P=N} - n^{\pi}_{Cl}$	−8.13 $(n_N - n_P) - n_{Cl} + \sigma_{iso}$
−8.12 $n^{\perp}_{Cl} - (n_{As} + n_N)$	−8.19 $(n_N + n_P) - n_{Cl}$	−8.31 $(n_N + n_P) - n_{Cl}$	−8.45 $\pi_{P=N} - n^{\pi}_{Cl}$
−8.66 $\sigma_{SiC}, n^{\sigma}_{Cl}$	−8.78 $\sigma_{SiC}, n^{\sigma}_{Cl}$	−9.03 $\sigma_{SiC}, n^{\pi}_{Cl}$	−8.51 $n^{\perp}_{Cl}$
−8.72 $\sigma_{SiC}, n^{\pi}_{Cl}$	−8.85 $\sigma_{SiC}, n^{\pi}_{Cl}$	−9.04 $\sigma_{SiC}, n^{\sigma}_{Cl}$	−9.30 $\sigma_{SiC}, n^{\pi}_{Cl}$
−9.56 $\pi_{As=N} + n^{\pi}_{Cl}$	−10.05 $\pi_{P=N} + n^{\pi}_{Cl}$	−10.19 $\pi_{P=N} + n^{\pi}_{Cl}$	−9.37 σ_{SiC}
Ionic state energies (in eV)			
9.31 A′ $(n_N - n_{Cl})$	9.43 A′ $(n_N - n_P)$	9.65 A′ $(n_N - n_P)$	9.27 A′ $(n_N - n_P)$
9.68 A′ $(\pi_{As=N} - n^{\pi}_{Cl})$	10.00 A″ $(\pi_{P=N} - n^{\pi}_{Cl})$	10.18 A″ $(\pi_{P=N} - n^{\pi}_{Cl})$	10.41 A″ $(\pi_{P=N} - n^{\pi}_{Cl})$

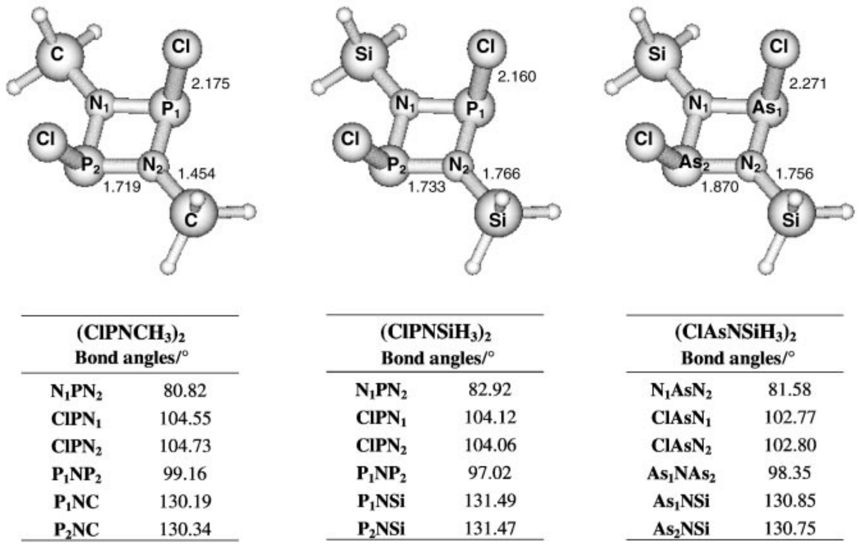

$(ClPNCH_3)_2$ Bond angles/°	
N_1PN_2	80.82
$ClPN_1$	104.55
$ClPN_2$	104.73
P_1NP_2	99.16
P_1NC	130.19
P_2NC	130.34

$(ClPNSiH_3)_2$ Bond angles/°	
N_1PN_2	82.92
$ClPN_1$	104.12
$ClPN_2$	104.06
P_1NP_2	97.02
P_1NSi	131.49
P_2NSi	131.47

$(ClAsNSiH_3)_2$ Bond angles/°	
N_1AsN_2	81.58
$ClAsN_1$	102.77
$ClAsN_2$	102.80
As_1NAs_2	98.35
As_1NSi	130.85
As_2NSi	130.75

Scheme 3 Geometrical parameters for the preferred structures of the silylated and alkyl dimeric species $(ClPnNXH_3)_2$ (X = C, Si). Bond lengths are given in Å.

Table 6 Calculated Kohn–Sham energies, ionic state energies and assignment of the molecular orbitals for the $(ClPnNSiH_3)_n$ [Pn = P, As; n = 1, 2] and $(ClPNCH_3)_2$ preferred geometries

$ClAs{=}NSiH_3$	$(ClAsNSiH_3)_2$	$ClP{=}NSiH_3$	$(ClPNSiH_3)_2$	$(ClPNCH_3)_2$
Kohn–Sham energies (in eV) and assignment of molecular orbitals				
-7.89	-7.61	-7.86	-7.49	-7.28
$n_N - n_{Cl}^{\sigma}$	$n_{As}{}^{-}$	$n_N - n_P - n_{Cl}^{\sigma}$	$n_P{}^{-}$	$n_P{}^{-}$
-8.32	-7.71	-8.53	-7.67	-7.40
$\pi_{As=N} - n_{Cl}^{\pi}$	$n_N{}^{+}$	$n_P + n_N - n_{Cl}$	$n_N{}^{+}$	$n_N{}^{-}$
-8.46	-7.76	-8.59	-8.09	-7.42
$n_{As} - n_{Cl}^{\sigma}$	$n_N{}^{-}$	$\pi_{PN} - n_{Cl}^{\pi}$	$n_N{}^{-}$	$n_N{}^{+}$
-9.36	-8.62	-9.68	-8.79	-8.59
$\pi_{As=N} + n_{Cl}^{\pi}$	n_{Cl}	$\pi_{PN} + n_{Cl}^{\pi}$	n_{Cl}	n_{Cl}
-9.40	-8.67	-9.72	-8.87	-8.65
$n_{As} + n_N + n_{Cl}$	n_{Cl}	$n_P + n_N + n_{Cl}$	n_{Cl}	n_{Cl}
-10.50	-8.96	-10.91	-9.24	-8.98
n_N, σ_{SiH}^{π}	n_{Cl}	$\pi_{PN} + n_{SiH}^{\pi}$	n_{Cl}	n_{Cl}
Ionic state energies (in eV)				
9.95	9.43	10.02	9.30	9.20
A′ $(n_N - n_{Cl})$	$n_{As}{}^{-}$	A′ $(n_N - n_P - n_{Cl})$	$n_P{}^{-}$	$n_P{}^{-}$
10.34	—	10.75	—	—
A″ $(\pi_{As=N} - n_{Cl})$		A″ $(\pi_{PN} - n_{Cl}^{\pi})$		

ionizations, which correspond to the chlorine lone pairs and σ_{SiC} orbitals with the same symmetry, is about 0.7 eV.

Thus, if we experimentally observe the monomeric species, we can expect for the phosphorus and arsenic compounds a first band around 9.3 eV associated with the $n_N - n_{Pn}$, σ_{PnCl} and σ_{PnCl}^{*} orbitals, a second one around 10 eV with two ionizations from the $\pi_{Pn=N}$ and the $n_N + n_{Pn}$, $\sigma_{Cl(peri)}$ orbitals and a third band, more separated, which corresponds to the σ_{SiC} and n_{Cl} orbitals.

As the formation of the dimeric species [2 + 2] cannot be excluded without performing a complete theoretical study of these compounds, we carried out calculations on both $[ClPN(SiH_3)_2]_2$ and $[ClAsN(SiH_3)_2]_2$. Previously, the [2 + 2] cyclo-dimers $[ClPN^tBu]_2$ [9b] and $[ClAsN^tBu]_2$ [15] have been isolated and their X-ray structures show almost planar rings with two chlorine atoms in *cis* positions. The photoelectronic spectrum of $[ClPN^tBu]_2$ recorded by Walther[9b] presents a broad band at 9 eV.

We performed a theoretical study on this dimer, replacing the *tert*-butyl group with a methyl, in order to check if the theoretical method and the basis set used provide ionization energies in agreement with the experimental values. We found the lowest energy structure with the two chlorine atoms lying on the same side of the $(PN)_2$ plane, as revealed in the X-ray structure (Scheme 3). We present in Table 6 the calculated Kohn–Sham energies. The ionizations of the nitrogen and phosphorus lone pair combinations are energetically very close. The first ionic state is calculated to be at 9.2 eV. By taking into account the destabilizing effect of the *tert*-butyl group, the ionizations of this system are reasonably well approximated. For the studied silylated dimeric species, the structure with two chlorine atoms *cis* is also energetically preferred (Scheme 3). The energy difference between this geometry and that with two chlorine atoms *trans* is about 1.04 (As)–2.35 kcal mol^{-1} (P). We present in Table 6 the Kohn–Sham energies for these isomers and make a comparison with the values of the monomeric species. For the dimeric compounds, we have also calculated the first ionic state energy, which is associated with the antibonding combination of lone pairs of the pnictogen. It lies about 0.5–0.7 eV lower than that of the monomeric derivative. The Kohn–Sham energies for the nitrogen lone pairs are calculated to be very close to the HOMO for As and more separated for P. The subsequent ionizations correspond to the chlorine lone pairs and their Kohn–Sham energies are higher than those of the monomeric compounds.

Interpretation of the experimental spectra

For $ClAs{=}NSiMe_3$ (**1b**), the first two ionization energies are calculated to be at 9.3 and 9.7 eV (Table 5). If we look at the Kohn–Sham energies, the third Kohn–Sham orbital is energetically very close to the second and thus these two ionizations will appear at about the same energy. The theoretical data are in agreement with the experimental observations [Fig. 3(a)] since we observed a first band at 9.2 eV and a second more intense one at 9.8 eV. The fourth Kohn–Sham energy is shifted about 0.5–0.6 eV with respect to the third one, which is consistent with the experimental band observed at 10.6 eV. Consequently, the first thermolysis spectrum of $Cl_2AsN(SiMe_3)_2$ (573 K) can be assigned, without ambiguity, to the monomeric species $ClAs{=}NSiMe_3$. The ionization at 9.2 eV corresponds to the removal of an electron from the $n_N - n_{As}$ orbital mixed with the σ_{AsCl} and σ_{AsCl}^{*} orbitals and that at 9.8 eV is associated with the ionization of the π_{AsN} orbital mixed with the chlorine lone pair in the same plane and to the bonding combination of lone pairs $n_N + n_{As}$ mixed with n_{Cl} (high weight on As and Cl). The band at 10.6 eV is attributed to the ionizations of the chlorine lone pairs and the σ_{SiC} orbitals.

The difference between the first calculated ionization energy of $ClAs{=}NSiH_3$ (9.95 eV) and $(ClAsNSiH_3)_2$ (9.48 eV) is about 0.5 eV. By comparison with $ClAs{=}NSiMe_3$ (expt. value: 9.2 eV), we expect for the dimeric species $(ClAsNSiMe_3)_2$ a first band at about 8.7 eV. A calculation performed on $(ClAsNSiH_3)_2$ shows that the first three Kohn–Sham orbitals are the antibonding combination of lone pairs of arsenic ($n_{As}{}^{-}$), the bonding combination of lone pairs of nitrogen ($n_N{}^{+}$) and the antibonding one ($n_N{}^{-}$) (Table 6). By taking into account the greater destabilizing effect of the $SiMe_3$ group compared to SiH_3, stronger on the second and third ionizations (silyl group linked to N), the first experimental band should correspond to three ionizations: $n_{As}{}^{-}$, $n_N{}^{+}$ and $n_N{}^{-}$ and the energy gap to the second band should be more important. Thus, the spectrum recorded at 1223 K can be assigned to the formation of the dimeric species $(ClAsNSiMe_3)_2$. The first broad band centered on 8.9 eV corresponds to the ionization of electrons of $n_{As}{}^{-}$, $n_N{}^{+}$ and $n_N{}^{-}$. The second, more intense, band at 10.6 eV is associated with the ionization of electrons of the chlorine lone pairs. Nevertheless, we cannot exclude the presence of the monomeric species $ClAs{=}NSiMe_3$ under these first two bands (presence of ionizations at 9.2 and 9.8 eV).

In comparison with the experimental values for $(ClAsNSiMe_3)_2$, we can expect for the dimer $(ClPNSiMe_2{}^tBu)_2$ a first ionization lower than 8.9 eV because of the destabilizing effect of the *tert*-butyl group. Thus, the compound observed after thermolysis of $Cl_2PN(SiMe_2{}^tBu)_2$ and characterized by two first bands at 9.3 and 10.5 eV [Fig. 2(d)] cannot be the dimer $(ClPNSiMe_2{}^tBu)_2$. Considering our experimental conditions as well as the loss of $Me_2{}^tBuSiCl$, the formation of the monomer $ClP{=}NSiMe_2{}^tBu$ can be proposed looking at Table 5 (ΔSCF energies), it can be seen that, for the phosphorus, the most important difference is between the energies of the first (A′) and the second (A″) ionic states. Therefore we would expect to experimentally observe two more widely separated bands for $ClP{=}NSiMe_2{}^tBu$ than for $ClAs{=}NSiMe_3$; this is in agreement with the experimental values: $ClAs{=}NSiMe_3$ (9.2 and 9.8 eV) and $ClP{=}NSiMe_2{}^tBu$ (centered on 9.3 and 10.5 eV). We calculate for $ClP{=}NSiH_2{}^tBu$ two first Kohn–Sham orbitals that are similar in energy, corresponding to the antibonding combination of lone pairs of phosphorus and nitrogen in interaction with the σ_{SiC} and n_{Cl} orbitals $[(n_N - n_P) - n_{Cl} - \sigma_{SiC}$ and $(n_N - n_P) - n_{Cl} + \sigma_{SiC}]$.

Moreover, the first ionic state A′ $[(n_N - n_P) - n_{Cl} - \sigma_{SiC}]$ of $ClP{=}NSiH_2{}^tBu$ is calculated to lie at 9.27 eV. So, by taking into account the weak destabilizing effect of the methyl groups ("buttressing effect"), the first experimental ionization at 9.2 eV can be assigned to the ejection of an electron from this state. The second experimental ionization at 9.4 eV (same band) is associated with the ionization of the $(n_N - n_P) - n_{Cl} + \sigma_{SiC}$ since the two Kohn–Sham energies are very close. The shoulder at 10.2 eV is attributed to the ionization of the $\pi_{P=N}$ orbital and the sharp band at 10.5 eV to the ionization of the chlorine lone pair (n_{Cl}) orbitals. Consequently, the spectrum observed from the thermolysis of $Cl_2PN(SiMe_2{}^tBu)_2$ corresponds to $ClP{=}NSiMe_2{}^tBu$.

The experimental ionization energies of $ClAs{=}NSiMe_3$ are consistent with those of $ClP{=}NSiMe_2{}^tBu$. Indeed, the antibonding combination of lone pairs $n_N - n_{Pn}$ of $ClP{=}NSiMe_2{}^tBu$ and $ClAs{=}NSiMe_3$ appears at about the same ionization potential. In contrast, the ionization energy of the $\pi_{P=N}$ orbital is higher than the one of $\pi_{As=N}$ (better overlap for the phosphorus).

Conclusions

Contrary to the azo compounds (–N=N–),[16] the phosphaimines and arsaimines have not been extensively studied because of the kinetic instability of these species due to the high reactivity of the π_{PnN} bond ([2 + 1] and [2 + 2] dimerizations). Nevertheless, the coupled technique of FVT-PES allowed us to generate and characterize for the first time in the gas phase two new group 15 low-coordinate species. $ClAs{=}NSiMe_3$ and $ClP{=}NSiMe_2{}^tBu$ present an energetically preferred *cis* form. One of the main reasons for the thermodynamic stabilization of these halogeno systems appears in the important antiperiplanar interactions between the nitrogen lone pair and the σ^*_{AsCl} (or σ^*_{PCl}) bond and in the high polarity of the AsN bond due to the Cl atom. Despite the $SiMe_3$ and $SiMe_2{}^tBu$ substituents linked to N, which lead to a stabilization of the π system by negative hyperconjugation with the σ^*_{SiC} orbitals,[17] the π system of the –Pn=N– moiety (9–10 eV) remains more unstable than –N=N– (11 eV).

In order to provide a new description of these π bonds containing heavy atoms, a topological analysis of the electron localization function (ELF)[18] in these derivatives is in progress.

Computational details

Ab initio calculations were performed with the GAUSSIAN 94 program.[19,20] The density functional method[21] used was the hybrid exchange B3LYP functional.[22] This functional includes a linear combination of a small amount (20%) of exact exchange with the Becke 88 gradient-corrected exchange[22a] and with the LYP correlation energy functional:[22c]

$$E_{xc} = aE_x^{HF} + bE_x^{LDA} + cE_x^{GGA} + dE_c^{LDA} + eE_c^{GGA}$$

Standard parameterizations have been retained ($a = 0.20$, $b = 1 - a$, $c = 0.72$ for the Becke exchange, $e = 0.81$ for the gradient-corrected part of the correlation energy functional and $d = 1 - e$).

The 6-311G(d,p) set was retained as the basis set for all calculations, since the inclusion of polarization is necessary in order for accurate energies to be obtained. Geometry optimizations were performed and confirmed as true minima by frequency calculations.

We chose the B3LYP functional because we have previously checked that it leads to a satisfactory quantitative evaluation of the calculated ionization energies of heteroatomic molecules.[23] Ionization energies have been determined as the difference between the cation and the neutral molecule energies ($IE = E_{cation} - E_{molecule}$: ΔSCF method).

Moreover, the use of Kohn–Sham (KS) density functional theory (DFT) presents many advantages. First, the cost of a KS-DFT calculation is at most of the same order of magnitude as a Hartree–Fock computation, whereas most of the description of electron correlation is taken into account. Thus, it is substantially less expensive than traditional correlated techniques and so is very useful in our case for the calculations involving dimeric species or monomeric compounds with substituents such as $C(CH_3)_3$ or $SiMe_3$.

For large molecules, the correlation between ionization potential and Kohn–Sham energies calculated with common functionals (Koopmans' theorem-like) is largely discussed. Arduengo and co-workers[24] first used DFT calculations at the nonlocal level to assign their photoelectron spectra. They applied a uniform shift to the orbital energies, considering the difference between the calculated and experimental molecular ionization potential. The aim was to directly compare the KS energies to the experimental energies. Moreover, Werstiuk and Rademacher and their colleagues[25] have developed and successfully applied a routine for the interpretation of PE spectra based on B3LYP theory. This routine requires the calculation of the molecule's first vertical ionization potential IP_v. Calculated orbital energies $-\varepsilon$ are then shifted uniformly so that the HOMO energy equals that of the IP_v, giving the higher IPs. More recently, Stowasser and Hoffmann[26] confirmed that the KS orbitals are a good basis for qualitative interpretation of molecular orbitals. They concluded that if we want to go a step beyond a qualitative interpretation and look at orbital energies as rough ionization potentials, and if the DFT calculations are done with commonly used potentials, then it appears we must take the absolute constant and linear orbital energy shift into account by applying a suitable $ax + b$ scaling. In the case of large molecules, the ordering of levels found using the DFT calculations seems to be qualitatively well translated by using HF methods as well. This fact, despite the evident limits of correlation, gives a good base to discuss the ionization assignments, which cannot be reached by a direct calculation.

Experimental

Photoelectron spectra were recorded on a Helectros 0078 spectrometer equiped with a 127° cylindrical analyzer and monitored by a micro-computer supplemented with a digital–analog converter. The spectra were recorded with 21.21 eV HeI radiation as the photon source and calibrated on the well known auto-ionization of helium at 4.98 eV [$He^{II}(He)$] and those of nitrogen at 15.59 and 16.98 eV.

Two types of pyrolysis experiments, coupled with photoelectron spectroscopy, were performed. First, flash pyrolysis was effected inside the ionization chamber of the UV-PES spectrometer equipped with an internal heater device. The pressure of the ionization chamber was 10^{-5} mbar without sample. The first experiment, denoted "internal thermolysis", allowed the analysis of both species with short lifetimes and their decomposition products. The second system was an apparatus external to the spectrometer, which allowed a separate product study. Thermolysis was performed in a vacuum device (pressure in the oven: 10^{-5} mbar without sample) connected to the spectrometer. In this case only the stable and volatile species were characterized after cryogenic distillation. Unstable compounds decomposed and/or polymerized because of the long distance between the oven and the ionization head. Thermolysis temperatures varied between 300 and 1300 K depending on the compound being studied.

Compounds **1b** and **2a** were obtained by previously described methods.[27,28] **2b** was prepared from $(Me_2{}^tBuSi)_2NLi$ and $AsCl_3$ as described for **2a**.[29]

Acknowledgements

Financial support of this work by the CNRS (France) is gratefully acknowledged. We also thank the Institut du Developpement de Ressources en Informatique Scientifique (IDRIS, Orsay, France), administered by the CNRS, for the calculation facilities, and Dr Gijs Schaftenaar for allowing us to use his graphics program Molden.[30]

References and notes

1 K. Miqueu, J.-M. Sotiropoulos, G. Pfister-Guillouzo, A.-C. Gaumont and J.-M. Denis, *Organometallics*, 2001, **20**, 143.

2 (*a*) *Multiple Bonds and Low Coordination in Phosphorus Chemistry*, ed. M. Regitz and O. J. Scherer, Verlag, Weinheim, 1990, p. 13; (*b*) E. Niecke and D. Gudat, *Angew. Chem., Int. Ed. Engl.*, 1991, **30**, 217; (*c*) L. Weber, *Chem. Rev.*, 1992, **92**, 1839; (*d*) L. Weber, *Chem. Ber.*, 1996, **129**, 367.

3 (*a*) E. Niecke, D. Gudat, W. W. Schoeller and R. Rademacher, *J. Chem. Soc., Chem. Commun.*, 1985, 1050; (*b*) S. Elbel, A. Ellis, E. Niecke, H. Egsgaord and L. Carlsen, *J. Chem. Soc., Dalton Trans.*, 1985, 879; (*c*) G. David, V. Von Der Gonna, E. Niecke, T. Busch, W. W. Schoeller and R. Rademacher, *J. Chem. Soc., Faraday Trans.*, 1994, 2611.

4 (*a*) P. Hitchcock, M. F. Lappert, A. K. Rai and H. D. Williams, *J. Chem. Soc., Chem. Commun.*, 1986, 1633; (*b*) H. G. Ang and F. K. Lee, *Polyhedron*, 1989, **8**, 2331; (*c*) S. K. Vasisht, M. Sood, P. K. Werma, T. Kaur and K. Usha, *Phosphorus, Sulfur Silicon Relat. Elem.*, 1990, **47**, 349; (*d*) J. Th. Ahlmann, A. Kunzel, H. W. Roesky, M. Noltemeyer, L. Markovskii and H. G. Schmidt, *Inorg. Chem.*, 1996, **35**, 6644; (*e*) C. Kruppa, M. Nieger, B. Ross and I. Väth, *Eur. J. Inorg. Chem.*, 2000, 165.

5 K. Miqueu, J.-M. Sotiropoulos, G. Pfister-Guillouzo and V. D. Romanenko, *Eur. J. Inorg. Chem.*, 2000, 477.

6 E. Niecke, F. Nieger and F. Reichert, *Angew. Chem., Int. Ed. Engl.*, 1988, **27**, 1715.

7 W. W. Schoeller, T. Busch and E. Niecke, *Chem. Ber.*, 1990, **123**, 1653.

8 E. Niecke and W. Bitter, *Syn. React. Inorg. Met.-Org. Chem.*, 1975, **5**, 231.

9 (*a*) S. Elbel and E. Niecke, *J. Chem. Soc., Dalton. Trans.*, 1985, 879; (*b*) H. Walther, Ph.D. Dissertation, Berlin, 1983.

10 (*a*) A. E. Reed, L. A. Curtiss and F. Weinhold, *Chem. Rev.*, 1988, **88**, 899; (*b*) J. P. Foster and F. Weinhold, *J. Am. Chem. Soc.*, 1980, **102**, 7211.

11 A. L. Allred and E. G. Rochow, *J. Inorg. Nucl. Chem.*, 1958, **5**, 264.

12 V. Métail, S. Joantéguy, A. Chrostowska-Senio, G. Pfister-Guillouzo, A. Systermans and J. L. Rippoll, *Main Group Chem.*, 1997, **2**, 97.

13 W. Ando, T. Ohtaki and Y. Kabe, *Organometallics*, 1994, **13**, 434.

14 S. Foucat, T. Pigot, G. Pfister-Guillouzo, H. Lavayssière and S. Mazières, *Organometallics*, 1999, **18**, 5322.

15 R. Bora, H. W. Roesky, M. Noltemeyer and G. M. Scheldrick, *Acta Crystallogr., Sect. C*, 1984, **40**, 1150.

16 (*a*) K. N. Houk, Y. M. Chang and P. S. Engl, *J. Am. Chem. Soc.*, 1975, **97**, 1824; (*b*) R. J. Boyd, J.-C. G. Bünzli and J. P. Snyder, *J. Am. Chem. Soc.*, 1976, **98**, 2398.

17 M. Ahmed and P. v. R. Schleyer, *J. Comput. Chem.*, 1994, **15**, 596.

18 (*a*) B. Silvi and A. Savin, *Nature*, 1994, **371**, 683; (*b*) A. Savin, R. Nesper, S. Wengert and T. F. Fassler, *Angew. Chem., Int. Ed. Engl.*, 1997, **36**, 1808.

19 M. J. Frisch, G. W. Trucks, H. B. Schlegel, P. M. W. Gill, B. G. Jonhson, M. A. Robb, J. R. Cheeseman, T. Keith, G. A. Petersson, J. A. Montgomery, K. Ragavachari, M. A. Al-Laham, V. G. Zakrzewski, J. V. Ortiz, J. B. Foresman, J. Cioslowswi, B. B. Stefanov, A. Nanayakkara, M. Challacombe, C. Y. Peng, P. Y. Ayala, W. Chen, M. W. Wong, J. L. Andres, E. S. Replogle, R. Gomperts, R. L. Martin, D. J. Fox, J. S. Binkley, D. J. Defrees, J. Baker, J. P. Stewart, M. Head-Gordon, C. Gonzalez and J. A. Pople, GAUSSIAN 94, Rev. C.3, Gaussian, Inc., Pittsburgh, PA, 1995.

20 W. J. Hehre, L. Radom, P. v. R. Schleyer and J. A. Pople, *Ab Initio Molecular Orbital Theory*, John Wiley and Sons, New York, 1986.

21 R. G. Parr and W. Yang, in *Functional Theory of Atoms and Molecules*, ed. R. Breslow and J. B. Goodenough, Oxford University Press, New York, 1989.

22 (*a*) A. D. Becke, *Phys. Rev. A*, 1988, **38**, 3098; (*b*) A. D. Becke, *J. Chem. Phys.*, 1993, **98**, 5648; (*c*) C. Lee, W. Yang and R. G. Parr, *Phys. Rev. B*, 1988, **37**, 785.

23 S. Joanteguy, G. Pfister-Guillouzo and H. Chermette, *J. Phys. Chem.*, 1999, **103**, 3505.

24 A. J. Arduengo III, H. Bock, H. Chen, M. Denk, D. A. Dixon, J. C. Green, W. A. Hermann, N. L. Jones, M. Wagner and R. West, *J. Am. Chem. Soc.*, 1994, **116**, 6614.

25 (*a*) H. M. Muchall and P. Rademacher, *J. Mol. Struct.*, 1997, **435**, 157; (*b*) H. M. Muchall and P. Rademacher, *J. Mol. Struct.*, 1998, **471**, 189; (*c*) H. M. Muchall, N. H. Werstiuk and B. Choudhurry, *Can. J. Chem.*, 1996, **76**, 221; (*d*) H. M. Muchall, N. H. Werstiuk, B. Choudhurry, J. Ma, J. Warkentin and J. P. Pezacki, *Can. J. Chem.*, 1998, **76**, 238.

26 R. Stowasser and R. Hoffmann, *J. Am. Chem. Soc.*, 1999, **121**, 3414.

27 M. J. S. Gynane, A. Hudson, M. F. Lappert, P. P. Power and H. Goldwhite, *J. Chem. Soc., Dalton. Trans.*, 1980, **12**, 2428.

28 E. Niecke, R. Rüger, M. Lysek, S. Pohl and W. W. Schoeller, *Angew. Chem., Int. Ed. Engl.*, 1983, **22**, 486.

29 B.p. 120 °C/0.2 mm Hg; ^1H NMR (80 MHz, $CDCl_3$): $\delta = 0.34$ [s, 12H, $Si(CH_3)_2$], 0.90 [s, 18H, ^tBu]; anal. calc. for $C_{12}H_{30}AsCl_2NSi_2$: C 36.92, H 7.75; found C 36.80, H 7.80%.

30 G. Schaftenaar and J. H. Noordik, *J. Comput.-Aided Mol. Des.*, 2000, **14**, 123.